Supporting Information for

CTAB Stabilizes Silver on Gold Nanorods

Weixiang Ye, Katja Krüger, Ana Sánchez-Iglesias, Isabel García, Xiaoyu Jia, Johannes Sutter, Sirin Celiksoy, Benjamin Foerster, Luis M. Liz-Marzán, Rubén Ahijado-Guzmán and Carsten Sönnichsen

Table S1. Particle Synthesis of single crystal gold nanorods. The amount of silver nitrate, seed solution and HCl was varied for the two different batches.

Particle solution	**$AgNO_3$ (4 mM)**	**Seed solution**	**HCl (37%)**
Batch 1 (Fig. 2 Red)	170 µL	15 µL	50 µL
Batch 2 (Fig. 2 Pink)	360 µL	16 µL	42 µL

Nanoparticle characterization. The nanoparticles were characterized by transmission electron microscopy (TEM). Figure S1 and S2 show representative TEM images of the two single crystal and the two penta-twinned batches respectively.

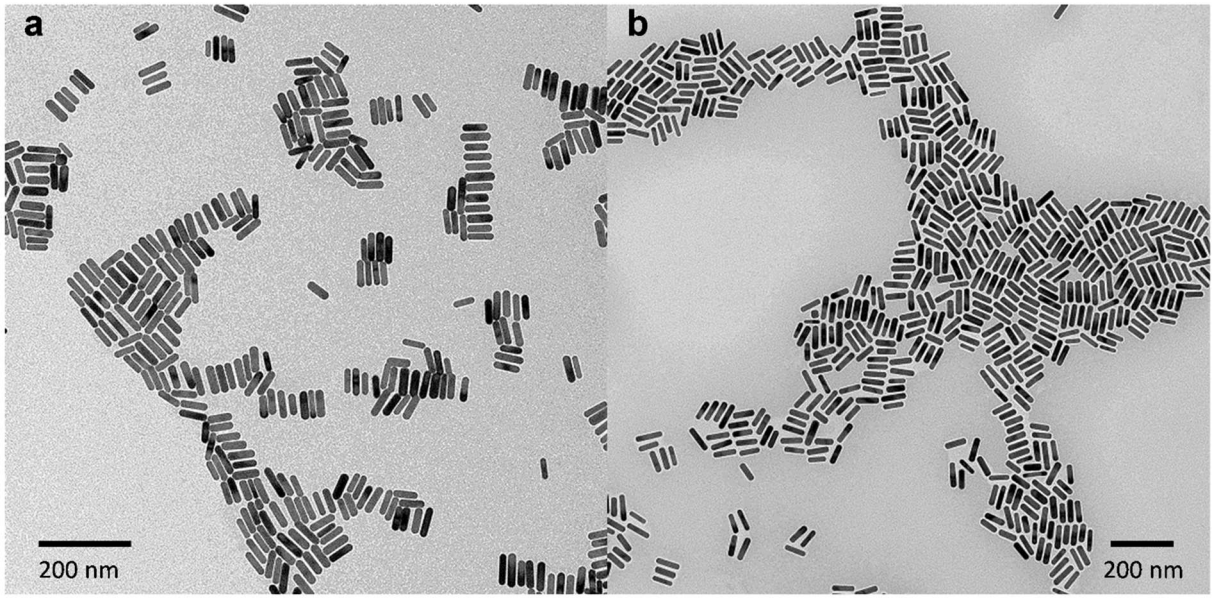

Figure S1. Representative TEM images of the single crystal batches of gold nanorods used in this work. **a**. Batch 1 (Fig. 2 red). Length of 59 ± 6 nm, width 16 ± 2 nm (Aspect ratio of 3.7) (mean value of 317 nanoparticles). **b**. Batch 2 (Fig.2, pink). Before washing the nanoparticles, they show a length of 66 ± 6 nm, and width of 17 ± 2 nm (Aspect ratio of 3.9). After washing the nanoparticles, the length was 64 ± 6 nm, and the width 17 ± 1 nm (Aspect ratio of 3.8). (Average values from around 1000 nanoparticles). These results allow us to discard any relevant morphological change during the process.

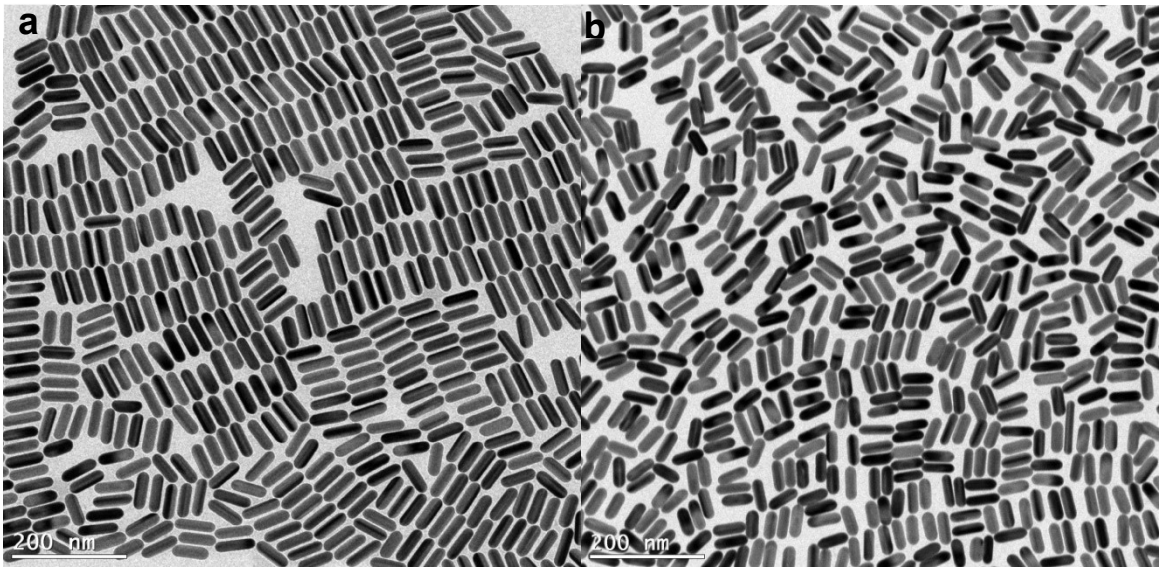

Figure S2. Representative TEM images of the pentatwinned gold nanorods. **a**. Batch 3 (Fig. 2 dark blue). Length of 66 ± 1 nm, width 19 ± 1 nm. **b**. Batch 4 (Fig. 2 light blue). Length of 57 ± 1 nm, width 18 ± 1 nm.

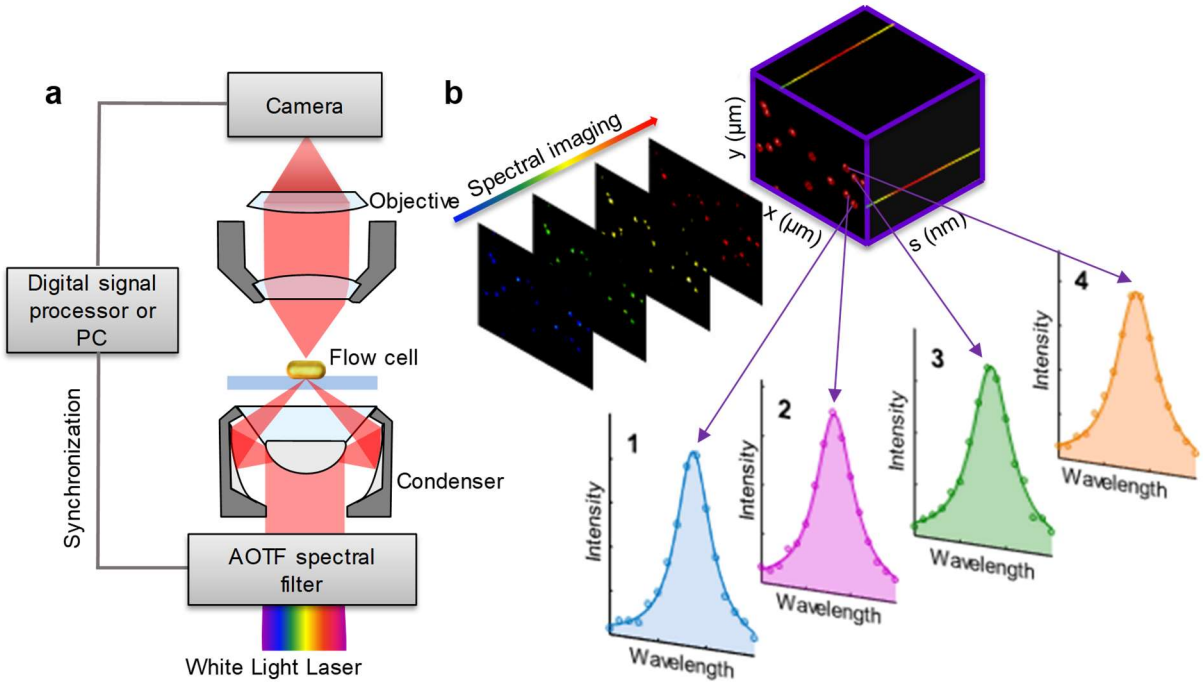

Figure S3. **a.** Microscope setup. The illumination is spectrally filtered by an acousto-optical tunable filter (AOTF), directed to the sample and recorded with a CMOS camera. **b**. The obtained images at different illumination wavelengths are combined to form a matrix (upper right). By using a home-made software, we identify and extract the spectra of all the particles in the field of view (see examples in the lower right corner, blue, pink, green and orange circles). From each spectrum, we determine the plasmon resonance wavelength λ_{res}, linewidth Γ and maximum intensity I_{max} by fitting with a Lorentzian function (lines).

Control experiments

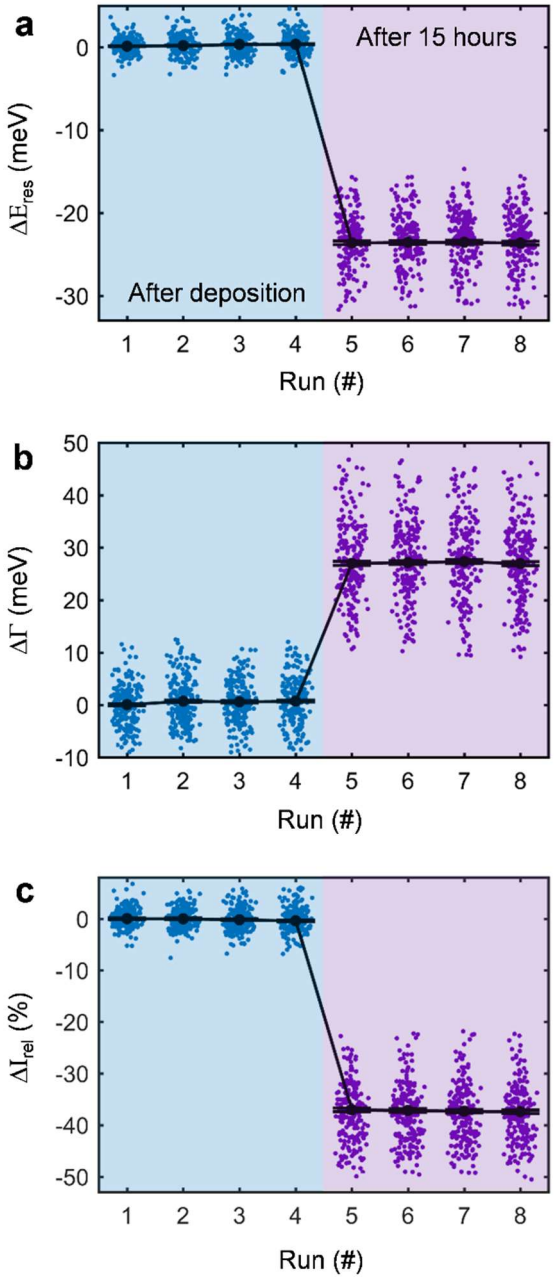

Figure S4. Response of the plasmon observables after washing the SC nanoparticles with water. The nanoparticle response was recorded after 15 hours under complete darkness to discard light-triggered effects. For this set of experiments, we used only SC gold nanorods. **a**. Plasmon resonance energy ΔE_{res}. **b**. Plasmon linewidth $\Delta\Gamma$. **c**. Relative scattering intensity ΔI_{rel}.

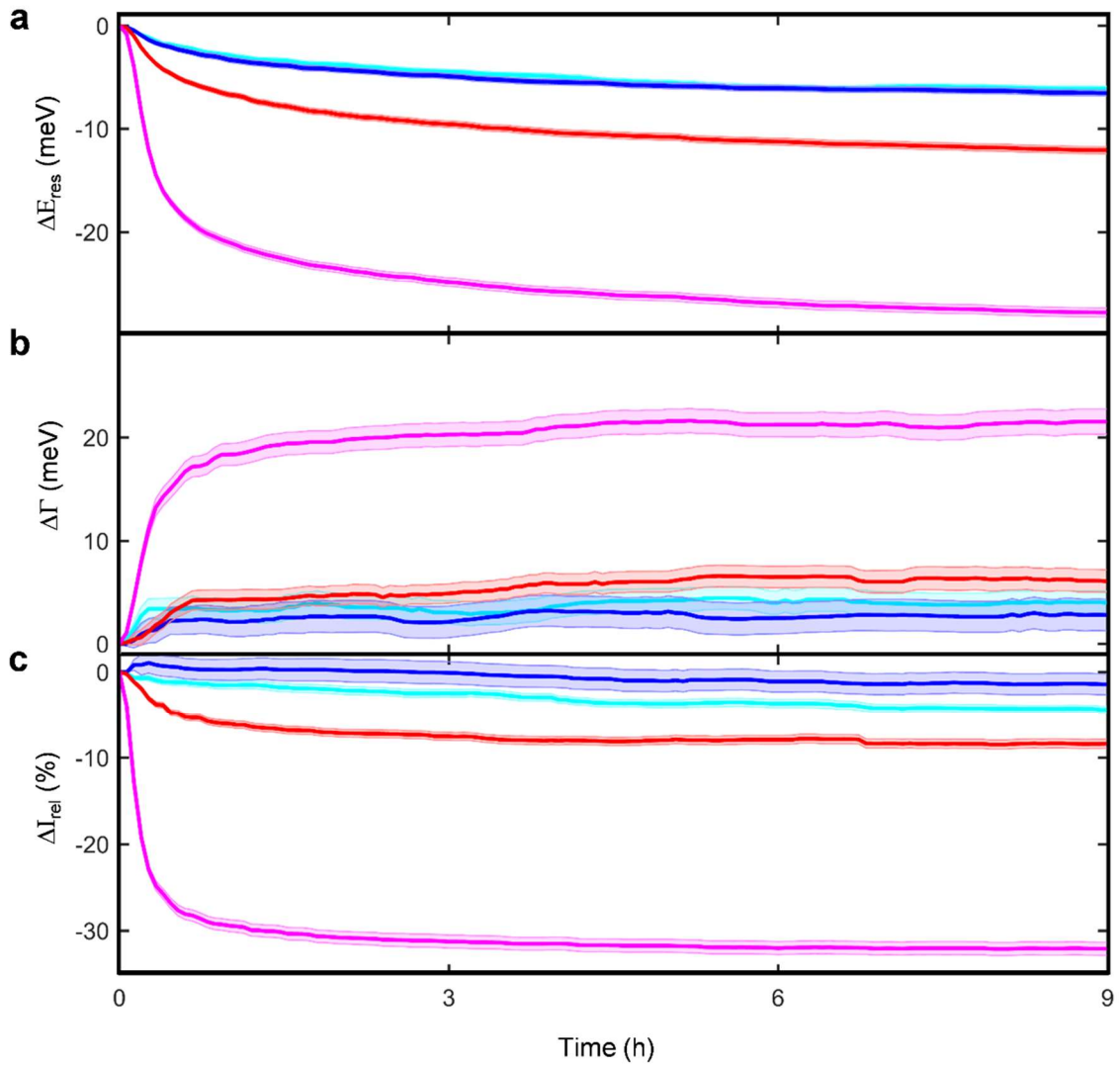

Figure S5. Change in the plasmon observables over time for two groups of PT gold nanorods (light and dark blue) and two groups of SC gold nanorods (red and pink). The evolution was recorded after washing the nanoparticles with ethanol for five minutes. **a**. Plasmon resonance energy ΔE_{res}. **b**. Plasmon linewidth $\Delta\Gamma$. **c**. Relative scattering intensity ΔI_{rel}.

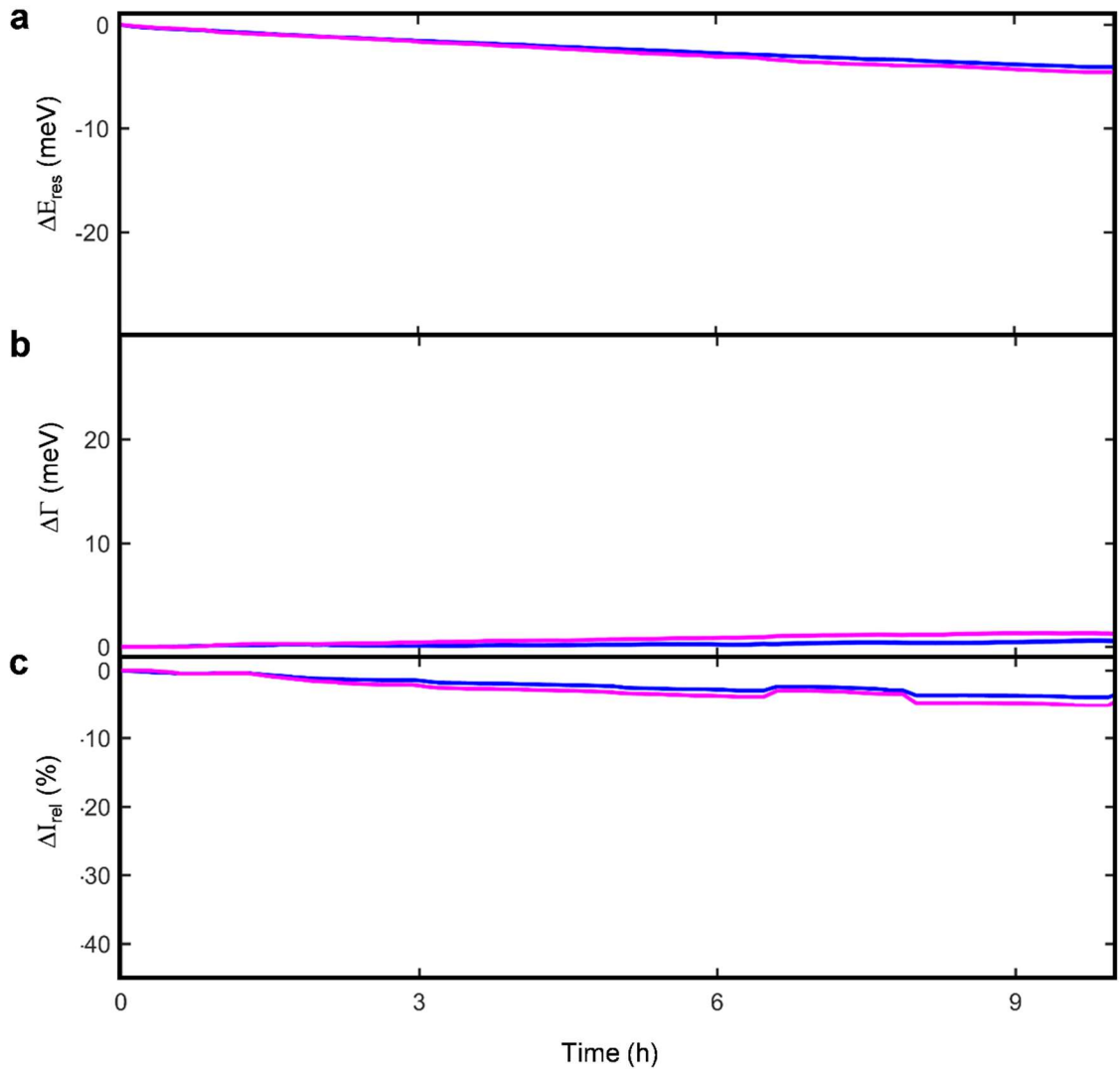

Figure S6. Change in the plasmon observables over time for two groups of PT gold nanorods (light and dark blue) and two groups of SC gold nanorods (red and pink). The evolution was recorded after washing the nanoparticles with non-polar mineral oil. **a**. Plasmon resonance energy ΔE_{res}. **b**. Plasmon linewidth $\Delta\Gamma$. **c**. Relative scattering intensity ΔI_{rel}.

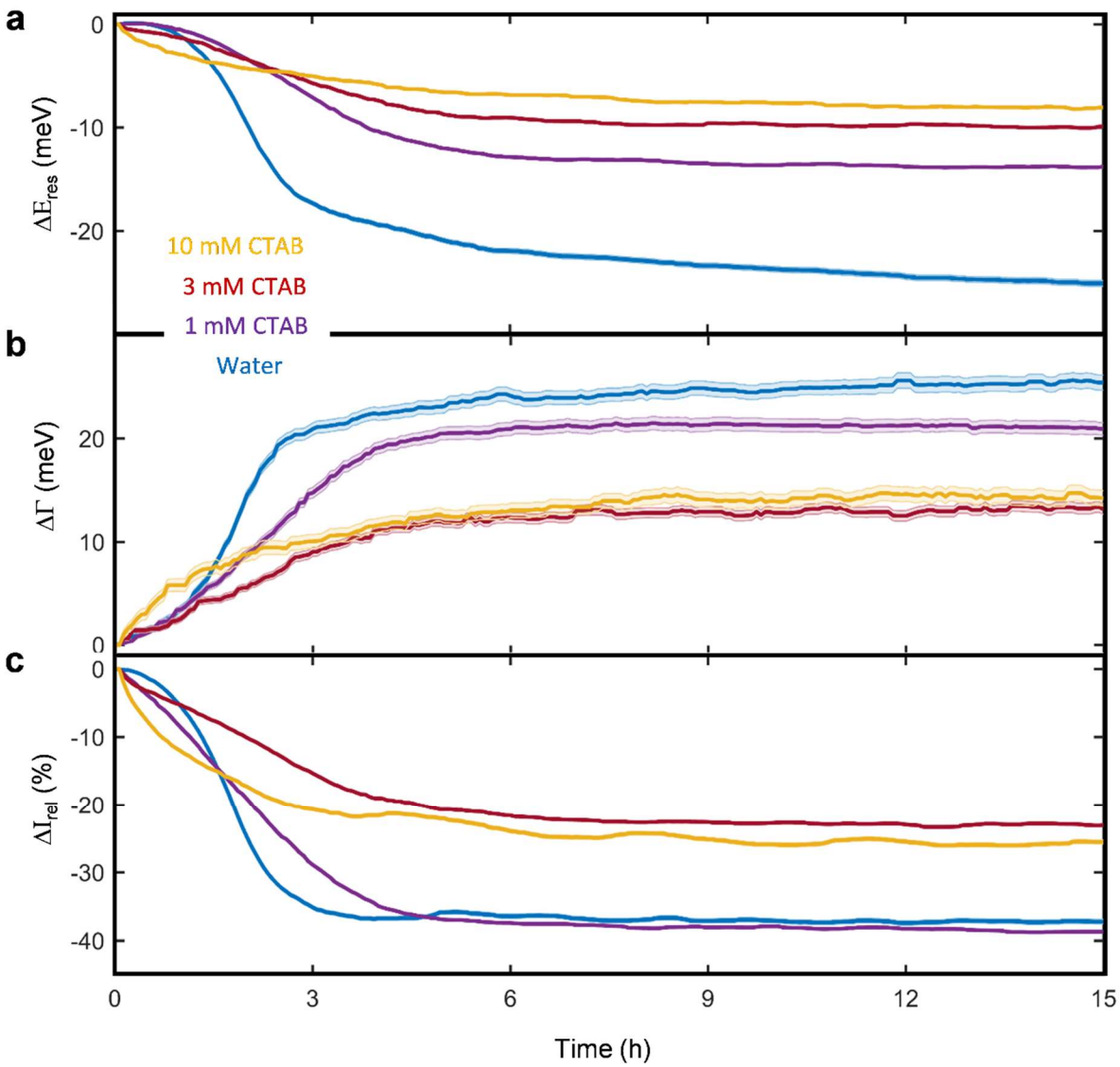

Figure S7. Change in the plasmon observables over time for SC gold nanorods. The evolution was recorded after washing the nanoparticles with solutions of CTAB at different concentrations. **a**. Plasmon resonance energy ΔE_{res}. **b**. Plasmon linewidth $\Delta\Gamma$. **c**. Relative scattering intensity ΔI_{rel}. Note that there is a change in the shape of the 'kinetic curve' at different CTAB concentrations. At high CTAB concentrations the CTAB surface density is higher (see reference 19 in the main text), and we expect an equilibrium between micelles in solution and micelles on the nanoparticles. This effect may however be suppressed at low CTAB concentrations, where the equilibrium would be shifted toward the solution.

X-ray photoelectron spectroscopy (XPS)

XPS was conducted on a Kratos Axis UltraDLD spectrometer (Kratos, Manchester, England) using an Al Kα excitation source with a photon energy of 1487 eV. XPS provides surface sensitivity with probing depth of 8–10 nm. The data were acquired in the hybrid mode using a 0° take-off angle, defined as the angle between the surface normal and the axis of the analyzer lens. XP spectra were collected with setting analyzer pass energy at 80 eV, and high-resolution spectra were collected with setting analyzer pass energy of 20 eV. Neutralizer was always used during spectra collection. Binding energy scales were calibrated to Au $4f_{7/2}$ emission at 84 eV.[1] The data was read and analyzed with the CasaXPS software.

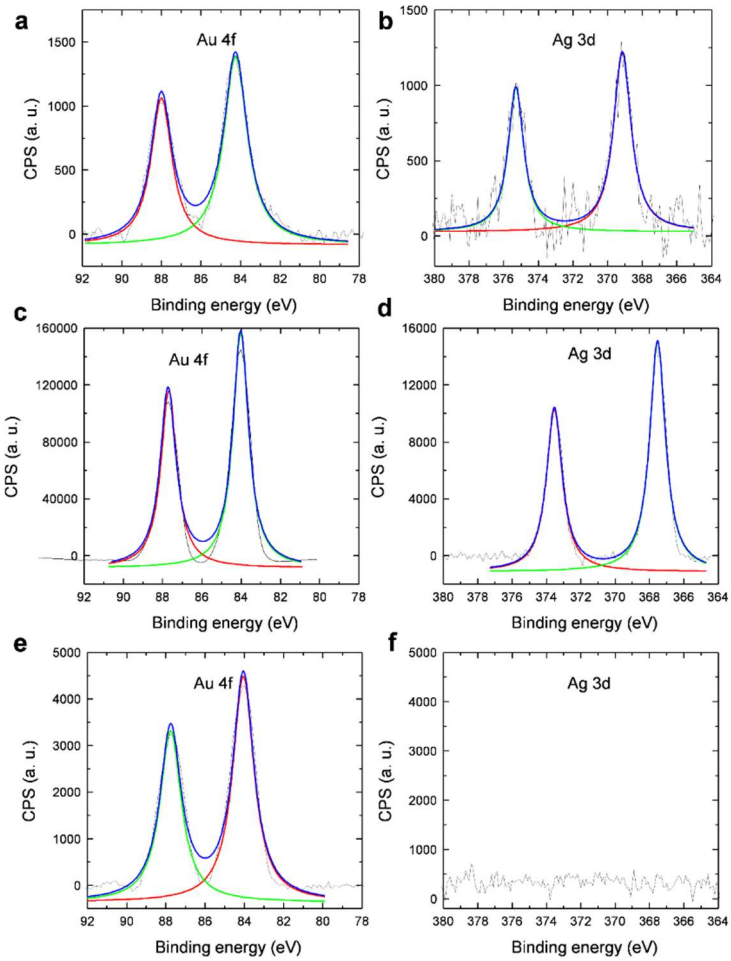

Figure S8. Representative Au 4f and Ag 3d XP spectra for Gold nanorods. **a**. Au 4f binding energy and **b**. Ag 3d for the SC gold nanorods before CTAB removal. **c**. Au 4f binding energy and **d**. Ag 3d for the SC gold nanorods after CTAB removal. Observe that the Ag 3d bands are shifted towards lower energies indicating that in this case silver might be Ag^+. **e**. Au 4f binding energy and **f**. Ag 3d for the PT gold nanorods. Before washing, the nanoparticles show an Auger parameter for silver of 722. After washing the nanoparticles, the Auger parameter for silver shifts to 718.5 indicating the silver oxidation in agreement with previous literature.[2]

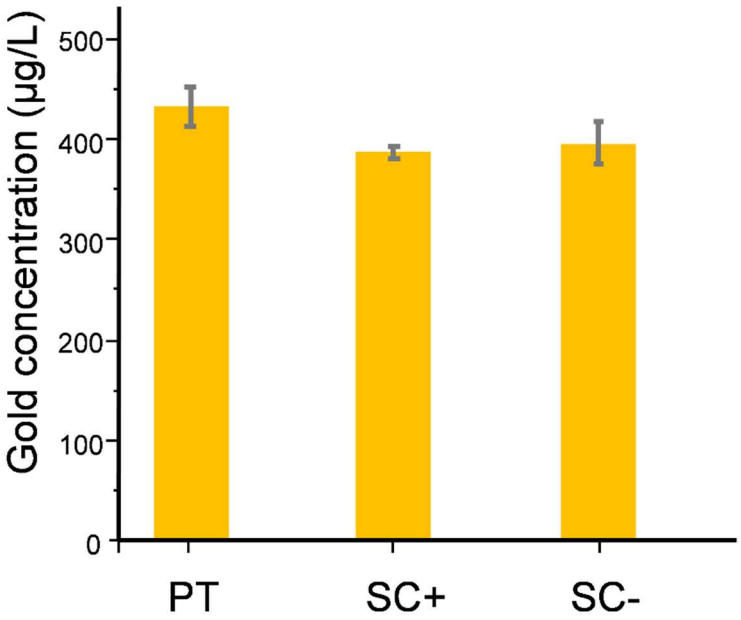

Figure S9. ICP-MS analysis of the PT and SC nanorods before, SC+, and after washing, SC- showing that after CTAB removal the gold concentration does not decrease.

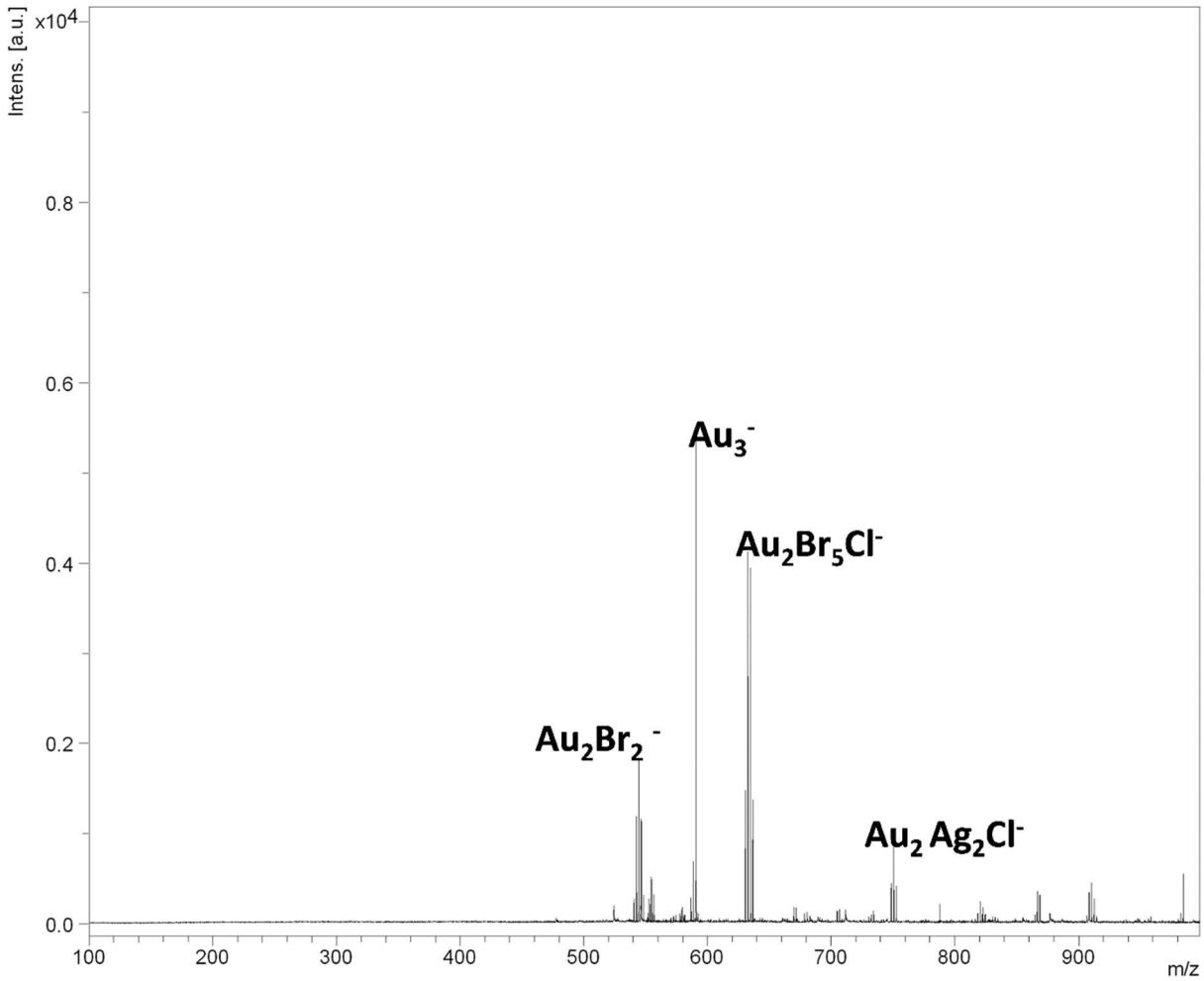

Figure S10. Mass spectrum of SC gold nanorods before CTAB removal.

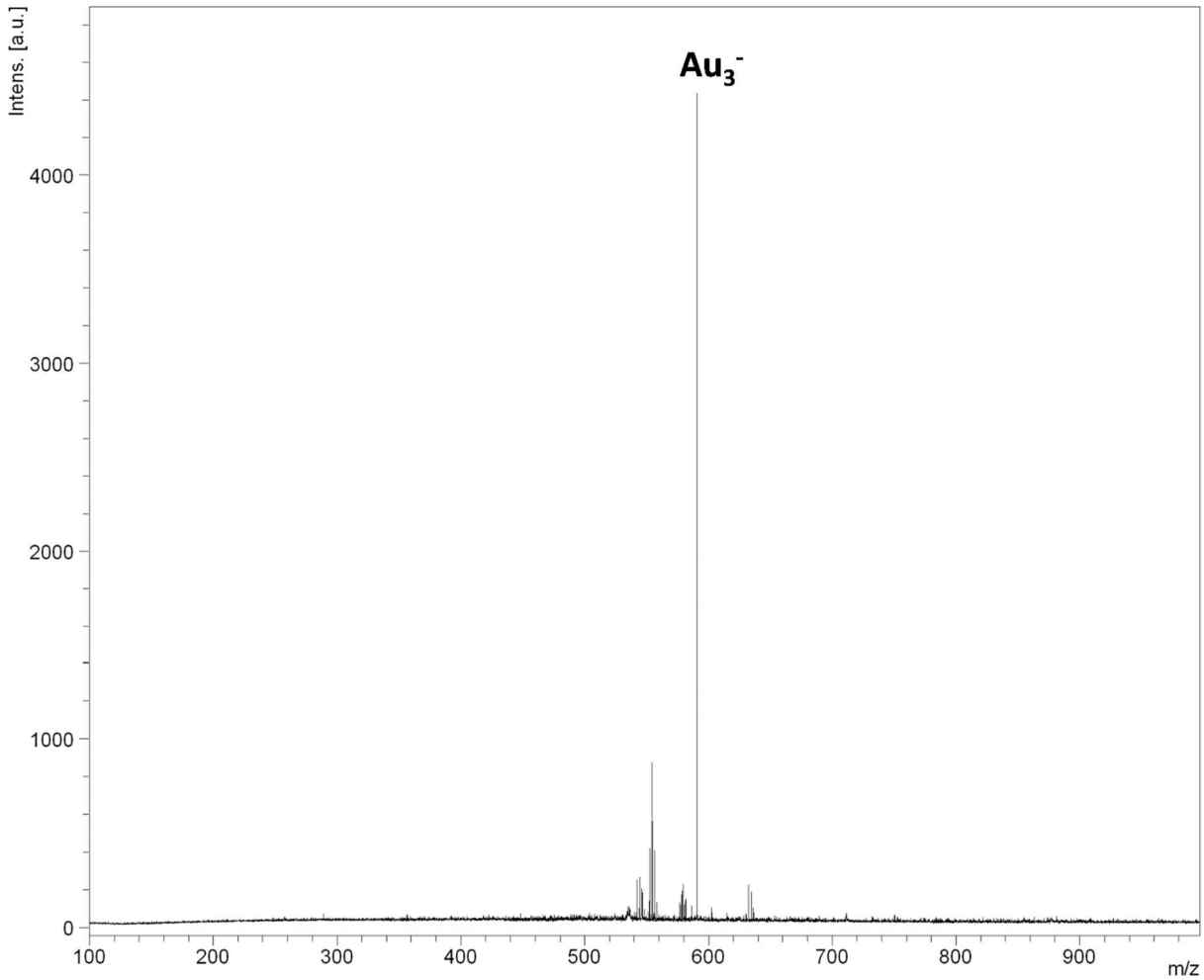

Figure S11. Mass spectrum of SC gold nanorods after CTAB removal.

References

1. Moulder, J. F., Chastain, J., Sobol, P. E., Bomben, K. D. Handbook of X-ray photoelectron spectroscopy. A reference book of standard spectra for identification and interpretation of XPS data. Physical Electronics Division, Perkin-Elmer Group: Eden Prairie, MN, USA, 1992.

2. Ferraria, A. M., Carapeto, A. P., Botelho do Rego, A. M. X-ray photoelectron spectroscopy: Silver salts revisited. *Vacuum* **2012**, *86*, 1988-1991.